CCFE
CULHAM CENTRE FOR FUSION ENERGY

UK Atomic Energy Authority

UKAEA-CCFE-CP(22)04

M.L. Richiusa, P. Ireland, J. Nicholas, Z. Vizvary

Rationale Behind EU-DEMO Limiter's Plasma-Facing Component Design Under Material Phase Change

Rationale Behind EU-DEMO Limiter's Plasma-Facing Component Design Under Material Phase Change

M.L. Richiusa, P. Ireland, J. Nicholas, Z. Vizvary

This paper has been submitted to
2021 IEEE Pulsed Power Conference & Symposium on Fusion Engineering (PPC/SOFE) NPSS, Denver, Colarado, USA, 12-16 December 2021

Rationale behind EU-DEMO limiter's plasma-facing component design under material phase change

M.L. Richiusa[a,b], P. Ireland[a], J. Nicholas[a], and Z. Vizvary[b]

[a]*Dept. of Engineering Science, University of Oxford, UK*
[b]*UKAEA-CCFE, Culham Science Centre, Abingdon, Oxon, OX14 3DB, UK*

***Abstract*— The protection strategy adopted for the European DEMOnstration (EU-DEMO) fusion power reactor foresees the use of sacrificial components – referred to as *limiters* – dealing with plasma-wall contacts. Their aim is to protect the first wall (FW) against the huge amount of plasma energy (up to GigaJoules) released in a few milliseconds during disruptive events, which might lead to melting and/or vaporization of the plasma-facing material. The current limiter design concepts rely on actively water-cooled plasma-facing components (PFC). As water is not allowed inside the main chamber, limiter's PFCs must be designed to preserve the cooling system integrity under any scenario, therefore the estimate of the thickness of material undergoing any phase change is crucial.**

Given the initial assessment of plasma magnetic configurations during off-normal events, this paper describes the procedure followed for designing the limiter's PFC, which includes a novel approach for estimating the molten thickness of material under high heat flux. A simplified 1D model has been implemented in Matlab, which deals with multi-phase moving boundary problems. This model takes its inspiration from the way phase change interface tracking problems are tackled in food industry (i.e. freeze-drying processes) and solute concentration diffusion-controlled problems. It overcomes the complexity of solving a strongly coupled non-linear system of partial and ordinary differential equations in moving spatial domains by adopting a change of coordinate system based on the Landau transformation. As a result, an equivalent and fixed spatial coordinate system is defined where the spatial domain boundaries of the different phases are constrained, and the systems of governing equations are easy to solve. Both the solid and liquid phases are modelled, while the vapour is assumed to be removed once formed. Its benchmark against computational results found in literature has shown a very good agreement, which paves the way to further development of it. For phase change interface tracking problems in 2D/3D and more complex geometries, a commercial Multi-physics software adopting the Lagrangian-Eulerian approach in moving mesh frames will be used for tackling problems where material is removed following a phase change. Although the vapour domain is not simulated, a set of gas kinetics boundary conditions couple the interface between vapour and liquid phases, driving its position over time. This will be detailed described in a future companion paper.

NOMENCLATURE

Acronyms

CQ	Current Quench
DVDE	Downward Vertical Displacement Event
DEMO	DEMOnstration fusion power plant
FW	First Wall
OLL	Outboard Lower Limiter
OML	Outboard Midplane Limiter
PDE	Partial Differential Equation
PFC	Plasma-Facing Component
RU/RD	Ramp-Up/Ramp-Down
SOF	Start-Of-Flat top
SOL	Scrape-Off Layer
TQ	Thermal Quench
UL	Upper Limiter
UVDE	Upper Vertical Displacement Event

Symbols

cp	Specific heat capacity, [J kg^{-1} K^{-1}]
H	Latent heat, [J m^{-3}]
HF	Heat flux, [W m^{-2}]
k	Thermal conductivity, [W m^{-1} K^{-1}]
L	Characteristic width, [m]
r	Liquid/vapour moving interface position, [m]
s	Solid/liquid moving interface position, [m]
t	Time, [s]
T	Temperature, [°C]
W	Tungsten
x	Current spacial coordinate, [m]

Subscripts

l	Liquid
m	Melting
max	Maximum
op	Operational
s	Solid
v	Vapour

Greek

ζ	Vapour phase domain spatial coordinate, [m]
η	Solid phase domain spatial coordinate, [m]
ξ	Liquid phase domain spatial coordinate, [m]
ρ	Density, [kg m^{-3}]
λ	SOL power fall-off decay length, [m]

I. INTRODUCTION

Together with plasma disruption mitigation strategies, special requirements are needed for preventing the plasma from touching the wall during both normal and disruptive events in future tokamaks. Unlike the existing experimental tokamaks, which work either without tritium or with lower plasma power levels, DEMO cannot operate safely with a bare tritium-breeding wall [1] as any plasma perturbation

could push its boundary towards the wall that will be severely damaged. Therefore, protruding protection panels (aka *limiters*) will be used for constraining the plasma boundaries. Limiters do not play any role in plasma stability. They are only meant to face plasma-wall impacts following unmitigated perturbations. Four different limiters are required to adequately protect the FW (see Fig. 2 in [1]):

- *OML* (4 in the 360° torus) for plasma RU/RD phases (see Fig.3 in [2]), and located at the outboard midplane. Plasma parameters: $P_{SOL} = 3.5$ MW in 35 sec, $\lambda = 6$ mm;
- *OLL* (4 in total) facing DVDEs (see Fig.5(lhs) in [2]) following vertical instabilities (caused by current or voltage value deviations from their reference ones), during which the plasma loses energy (TQ) while moving downwards, for then experiencing a CQ before disappearing. Plasma parameters during TQ: $P_{SOL} = 325$ GW in 4 msec, $\lambda = 7$ mm;
- *UL* (8 in total) facing UVDEs (see Fig.2 in [2]). Plasma parameters during TQ: $P_{SOL} = 325$ GW in 4 msec, $\lambda = 7$ mm;
- *IML* (4 in total) facing unforeseen transient events such as H-L transitions (i.e. going from high to low plasma performances, see Fig.5(rhs) in [2]). Plasma parameters: $P_{SOL} = 30$ MW in 5 sec, $\lambda = 2 - 4$ mm.

The limiter location overview is sketched in Fig.1 for a 2D DEMO FW cross-section, together with a summary of the charged particle HF_{max} experienced by every limiter during the transient it has to face, and the related exposure time.
Having given an overview on the European DEMO protection strategy, the present paper will briefly describe the work carried out for shaping the limiter plasma-facing surface in §II, before focussing on the approach adopted for phase change material thickness estimate to be included in the engineering design (§III-A). The resulting thermal model, with its analytical formulation, benchmark, and application, will be described and discussed in §III-A.1.

II. Limiter Plasma-Facing Surface Shaping

As plasma-surface interactions are hence concentrated on the limiter's plasma-wetted surface, they need to be suitably and safely designed for withstanding different loading conditions.
Although they are primarily designed for facing off-normal transients, edge-localized power deposition peaks should be avoided during the longest SOF. Because of the different plasma magnetic configurations, finding a unique surface shaping which spread the power deposition - due to charged particles spiralling along magnetic field lines - as even as possible during both SOF and transients is not straightforward, as the power deposition is described by an exponential law whose fall-off decay length is determined by λ. Hence, HF_{max} moves from the center of the surface (due to smaller λ values during disruptions) to the edges (for larger λ during SOF - see §I).
Each limiter's front faces has been designed by starting from a similar approach than the one used for ITER FW

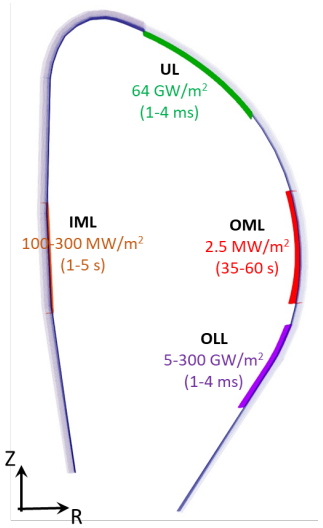

Fig. 1. Limiter heat load calculations due to charged particles during different plasma transients.

shaping [3], with the aim of finding a toroidal mid-plane profile that spread its related transient heat loads on as a large area as possible. The resulting logarithmic profile has been then adapted to the SOF magnetic configuration, by acting on the field-lines impinging angle. As a result of this iterative procedure carried out with field-lines tracing codes [4], chamfers have been implemented to the analytical shaping function of OLL, UL, and IML, obtaining the so called *2shape* profile (see Figs.2,3,4). Fig.5 shows the OML untouched logarithmic profile, which has proved to be suitable for both RU and SOF equilibria.

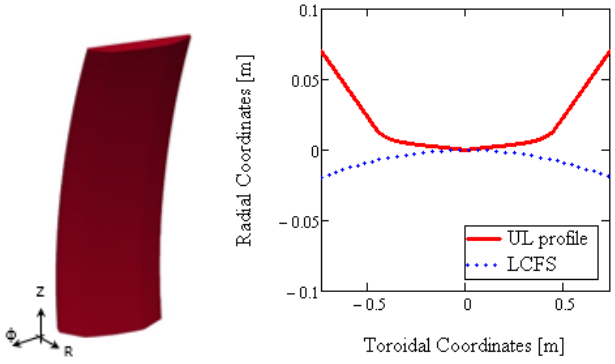

Fig. 2. UL plasma-facing surface (lhs) and its related toroidal 2shape profile (rhs).

III. Plasma-Facing Material Challenges

A. Multi-boundary layer approach for heat transfer problems involving changes of phase

Transient events can raise the temperature of the exposed surface up to the melting point and, eventually, to the boiling point. Metallic PFCs are prone to melting under heat loads in Fig.1, which can cause erosion and reduction of the PFC lifetime. Hence, the molten material amount estimate should

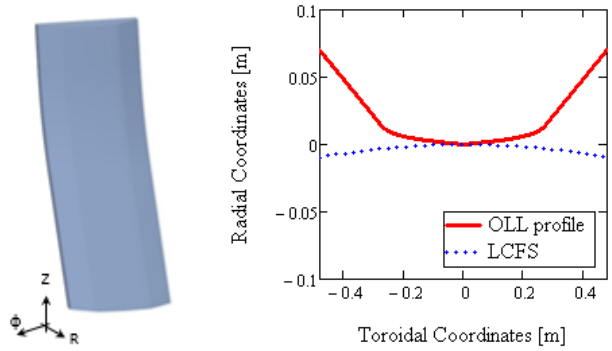

Fig. 3. OLL plasma-facing surface (lhs) and its toroidal 2shape profile (rhs).

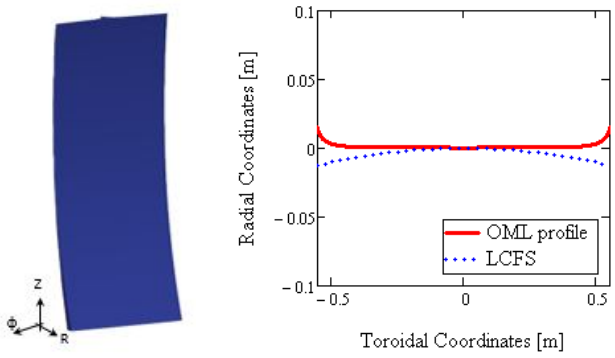

Fig. 5. OML plasma-facing surface (lhs) and its related toroidal profile (rhs).

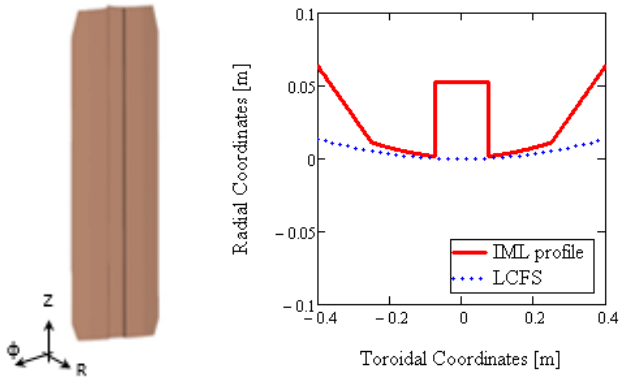

Fig. 4. IML plasma-facing surface (lhs) and its toroidal 2shape profile (rhs).

be design-driving, and included somehow in the PFC's finite element modelling and assessment.

The investigation of the heat transfer in solids involving a phase change falls within the Stefan-like problems [5], [6], which are characterized by interfaces between phases not known in advance. A moving interface is usually associated with time-dependent heat conduction problems described by the Fourier equation, a set of initial and boundary equations, and an additional energy balance equation (i.e. Stefan condition) imposed at the interface between phases. Their resolution describes both the time and space temperature trend in all the phase domains and the evolution of the inter-phase boundary positions. The Stefan condition makes the PDE system strongly non-linear as the time and space-evolution of the boundaries inherently depend on the calculated temperature. These problems are common in different research areas, i.e. casting solidification processes, food freezing, environmental engineering, ablation of missile skins under aerodynamic heating. Unfortunately, due to the non-linearity of the problem, exact analytical solutions are limited to single moving boundary problems (i.e. one of the two phases stays at phase change temperature) where the thermal problem is solved for only one phase [7]. For multiple moving boundary problems, the solution has to be found numerically.

For a zero-order estimate of the molten layer, a thermal model has been set up in Matlab solving the three different stages of heat transfer highlighted in Fig.6. A constant heat flux (HF) is applied at one face of a finite slab which is initially at uniform temperature below the melting point, whereas its back face is insulated.

The thermal model follows a staged-approach. The temperature rise is modelled until its font face reaches the melting point (triggering the beginning of the melting phase) and, eventually, the boiling point (beginning of the vaporization phase). The temperature distribution in the melted and unmelted portions of the slab, as well as the propagation of the melting layer, is therefore calculated.

1) Thermal model description: For simplifying the problem, the following assumptions are made:

- the solid material is considered to be pure, and the temperature at the interfaces is assumed constant and equal to the temperature of the phase changes (Fig.6);
- the solid is initially assumed to be at its isothermal temperature (T_{op});
- material properties are assumed constant within every phase but different between different phases;
- The vapour phase is assumed to be removed, once it appears;
- additional parameters are: (I) L: sample width; (II) k_s, k_l: solid and liquid phases thermal conductivity; (III) cp: solid and liquid phases specific heat capacity; (IV) H_m, H_v: latent heat of fusion and vaporization, respectively.

Three different systems of PDEs are solved for the three different stages:

- heating up phase: $0 \leq t \leq t_m$
  - Temperature values in the range $T_{op} \leq T \leq T_m$.
  - Spatial domain of the solid phase $0 \leq x \leq L$.

  The governing Fourier equation is:

$$k_s \frac{\partial^2 T_s(x,t)}{\partial x^2} = \rho c_p \frac{\partial T_s(x,t)}{\partial t} \qquad (1)$$

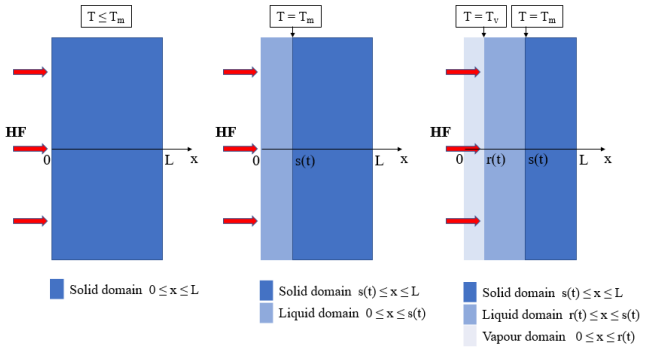

Fig. 6. Thermal model breakdown into the three main stages: heating up phase (lhs), melting phase (center) and vaporization phase (rhs).

with the following initial and boundary conditions:

$$T(x,0) = T_{op} \tag{2}$$

$$k_s \frac{\partial T_s}{\partial x}\Big|_{x=0} = -HF \tag{3}$$

$$k_s \frac{\partial T_s}{\partial x}\Big|_{x=L} = 0 \tag{4}$$

- melting phase: $t_m \leq t < t_v$
  - Temperature values in the range $T_m \leq T \leq T_v$.
  - Two spatial domains: (I) liquid $0 \leq x \leq s(t)$; (II) solid $s(t) \leq x \leq L$. This implies a solid/liquid interface moving boundary $s(t)$.

  The governing system of PDEs is:

$$k_l \frac{\partial^2 T_l(x,t)}{\partial x^2} = \rho c_p \frac{\partial T_l(x,t)}{\partial t} \quad @ \quad 0 < x < s(t) \tag{5}$$

$$k_s \frac{\partial^2 T_s(x,t)}{\partial x^2} = \rho c_p \frac{\partial T_s(x,t)}{\partial t} \quad @ \quad s(t) < x < L \tag{6}$$

  Considering the initial spatial temperature distribution the same as the resulting one from the heating up phase (Eq.7), the following initial conditions apply:

$$T_s(x,t_m) = T\,(x,t_m) \tag{7}$$

$$T_s(0,t_m) = T_m \tag{8}$$

$$s(t_m) = 0 \tag{9}$$

  together with the boundary conditions:

$$-k_l \frac{\partial T_l}{\partial x}\Big|_{x=s(t)} + k_s \frac{\partial T_s}{\partial x}\Big|_{x=s(t)} = \rho H_m \frac{ds(t)}{dt} \tag{10}$$

$$T_s(s(t),t) = T_l(s(t),t) = T_m \tag{11}$$

$$k_l \frac{\partial T_l}{\partial x}\Big|_{x=0} = -HF \tag{12}$$

- vaporization phase: $t \geq t_v$
  - Temperature values in the range $T \leq T_v$.
  - Three spatial domains: (I) vapour $0 \leq x \leq r(t)$; (II) liquid $r(t) \leq x \leq s(t)$; (III) solid $s(t) \leq x \leq L$. Two different interfaces are considered, i.e. vapour-to-liquid $r(t)$ and solid-to-liquid $s(t)$ moving boundaries.

The governing system of PDEs is the following:

$$k_l \frac{\partial^2 T_l(x,t)}{\partial x^2} = \rho c_p \frac{\partial T_l(x,t)}{\partial t} \quad @ \quad r(t) < x < s(t) \tag{13}$$

$$k_s \frac{\partial^2 T_s(x,t)}{\partial x^2} = \rho c_p \frac{\partial T_s(x,t)}{\partial t} \quad @ \quad s(t) < x < L \tag{14}$$

with the initial conditions listed below (by assuming the initial temperature distribution of the solid and liquid domains are the same as the resulting ones from the melting phase, i.e. Eq.15 and Eq.16, respectively):

$$T_s(x,t_v) = T\,(x,t_v) \tag{15}$$

$$T_l(x,t_v) = T\,(x,t_v) \tag{16}$$

$$r(t_v) = 0 \tag{17}$$

$$s(t_v) = s(t) \tag{18}$$

$$T_l(0,t_v) = T_v \tag{19}$$

and the following boundary conditions:

$$HF + k_l \frac{\partial T_l}{\partial x}\Big|_{x=r(t)} = \rho H_v \frac{dr(t)}{dt} \tag{20}$$

$$-k_l \frac{\partial T_l}{\partial x}\Big|_{x=s(t)} + k_s \frac{\partial T_s}{\partial x}\Big|_{x=s(t)} = \rho H_m \frac{ds(t)}{dt} \tag{21}$$

$$T_v(r(t),t) = T_l(r(t),t) = T_v \tag{22}$$

$$T_s(s(t),t) = T_l(s(t),t) = T_m \tag{23}$$

Taking into account moving boundary problems faced in freeze-drying [8] and solute concentration diffusion-controlled [9] processes, the Landau approach [10] simplifies the computational resolution of the problem. This is based on a transformation of the coordinate system by defining spatial variables (one for each phase) which, in turn, depend upon the moving interface. Although the transformation adds an additional complication inside the Fourier equation defined in every domain, it spatially constraints the phase domains between [0, 1]. Furthermore, their related spatial discretization takes into account the motion of the interface, which always falls in points where it is actually calculated. Consequently, any of the numerical methods developed to solve systems of PDEs can be used for solving the problem. The transformation introduces the following new spatial vari-

ables, which transform the PDEs listed above accordingly:

$$vapour\ domain: \zeta = \frac{x}{r(t)} \quad \Rightarrow \quad 0 \leq \zeta \leq 1 \tag{24}$$

$$liquid\ domain: \xi = \frac{x - r(t)}{s(t) - r(t)} \quad \Rightarrow \quad 0 \leq \xi \leq 1 \tag{25}$$

$$solid\ domain: \eta = \frac{x - s(t)}{L - s(t)} \quad \Rightarrow \quad 0 \leq \eta \leq 1 \tag{26}$$

2) Computational benchmark: The thermal model has been benchmarked against the results related to heat transfer problem involving heating and complete collapse of a solid wall through melting and heat transfer problem involving melting and partial vaporization of the liquid in [11]. The authors in [11] compare different algorithms (Finite Elements, Finite Differences, Boundary Elements) for solving the same multi-phase multiple boundary problem. For sake of brevity, the benchmark is shown only for the latter problem [11], although both the cases have given very promising results in terms of temperature evolutions (Fig.7), inter-phase boundary positions (Fig.8) and velocities (Fig.9). Although this simple

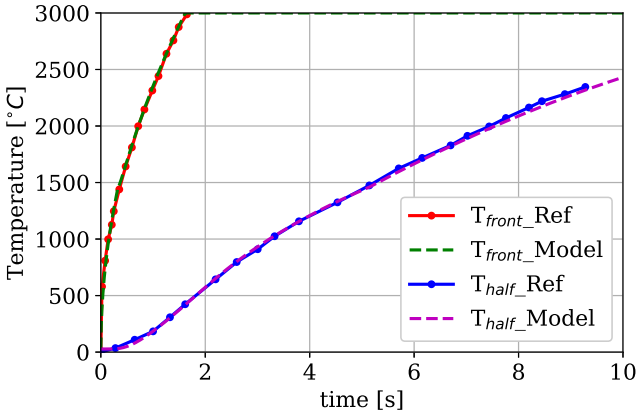

Fig. 7. Temperature evolution at the front face and at half thickness (L/2) of the 1D model.

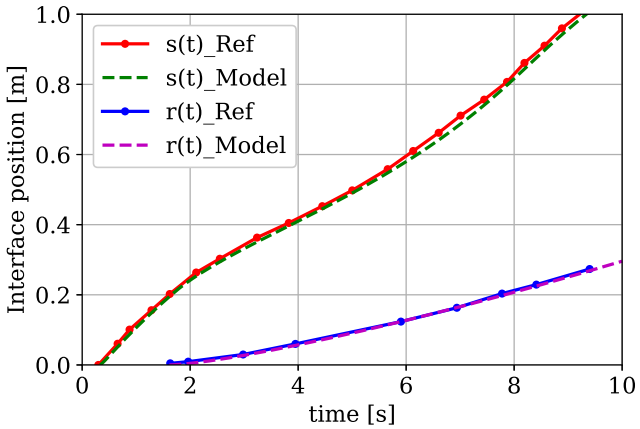

Fig. 8. Solid/liquid ($s(t)$) and liquid/vapour ($r(t)$) moving boundary tracking.

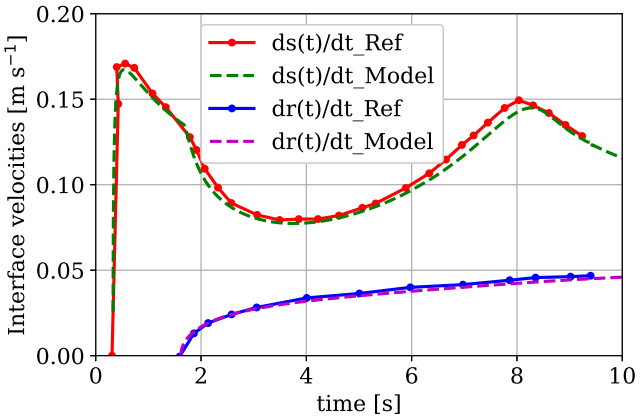

Fig. 9. Solid/liquid ($s(t)$) and liquid/vapour ($r(t)$) moving boundary velocities.

thermal model needs to be developed further, at this stage it has been applied for an estimate of the W molten thickness under heat loads generated by VDEs (Fig.1). In case of UVDE, a pure W slab undergoing a constant HF≈70 GW/m^2 for 4 ms experiences an instantaneous rise of its surface temperature (see Fig.10) up to the melting point (3422°C, @0.42μs), and, eventually, up to the boiling point (5660°C) in 2μs, producing a final melt and vapour thicknesses of, respectively, 4.5 mm and 4 mm. The same sudden temperature rise trend occurs under DVDE heat loads, although the huge amount of energy deposited on the surface brings it melting at 0.06μs and vaporizing in less than 1μs). At the end of the transient, the depth of the molten layer is ≈18 mm, of which unrealistic ≈17 mm are vaporized.

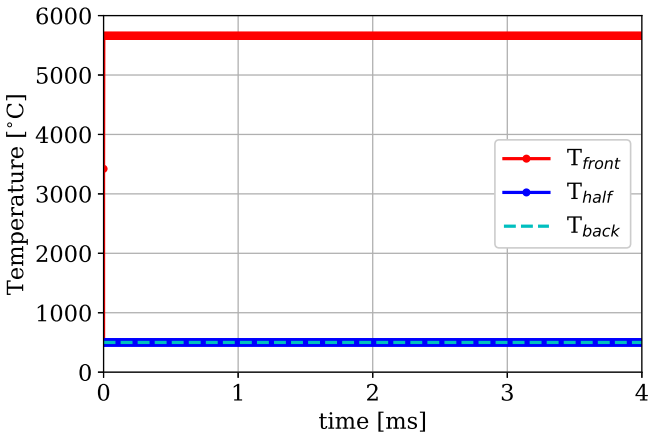

Fig. 10. Temperature evolution in a 1D finite slab of pure W withstanding the heat flux of a DVDE.

3) Result discussion and further work: The results obtained under VDE heat loads might not be realistically catching the physics governing the intense evaporation under vacuum, for at least two reasons: 1) the model represents the first attempt to tackle these kind of problems; 2) gas kinetics has not been taken into account in this zero-order thermal model for describing the vaporization phase, which

in its intense occurrence under vacuum conditions might not be well represented by a simple energy balance at the inter-phase. Despite this, the molten layer depth during UVDE appears to be of the same order of magnitude than the estimated molten thickness of $\approx$1100 μm in [12]. The temperature evolution in Fig.10 clearly shows that fast transients only affect the PFC surface. The TQ time scale is too short for letting the heat to diffuse across the sample thickness, therefore the PFC outermost layers only face the thermal wave by means of their material thermal inertia, leaving the rest of it at T_{op}. Provided that the molten thickness estimate is acceptable, this means that any cooling system located at least 20 mm far from the PFC surface should be considered unperturbed by the disruptive event. The Landau transformation is an easy way of overcoming the more complicated Lagrangian-Eulerian approach to the moving boundary problems, which require both more coding and computational efforts. The computational benchmark at low power level is promising, and it encourages a further development of the present thermal model approach after a deep dig on how the vaporization affects the heat transfer on the condensed phase, and whether any vapour shielding effect should be considered in the total amount of energy diffused across it. For sake of improving the knowledge gained so far, parallel studies on the two above-mentioned points are currently carried on by the aid of a Multi-physics software, and experiment planning is an additional feature which might help broaden the understanding on this topic. This will be illustrated in a future companion paper.

IV. CONCLUSIONS

Within the framework of EURO*fusion* DEMO First Wall and limiter design activities, the protection of the First Wall against power deposition peaks is one of the main criteria driving its design. Limiters are foreseen as sacrificial components for withstanding high heat fluxes following plasma-wall contacts in short timescale, preventing any FW irreversible damage. This feature makes the limiter design even more challenging as it should tackle non-conventional issues. If the shaping of their front face is needed for accommodating heat loads coming from different plasma magnetic scenarios, i.e. both off-normal transients and normal operations, the estimate of the potential melting depth is important for safety requirements raised by any water leakage inside the main vacuum chamber. Therefore, the integrity of the limiter cooling system should always been ensured. The aim of the present study is how the melting and vaporization erosion effects might be approached inside the design of a metallic PFC (especially limiters but easily extended to any PFC) directly exposed to plasma impact. It has appeared sensible tackling the issue as a multi-phase moving boundary problem, which is complicated by the appearance of interfaces whose movement is energy balance-driven. The way the thermal problem has been approached, and implemented in Matlab, takes the idea from the way the moving boundary problems are tackled in other technological processes (i.e. freeze-drying, solute concentration diffusion etc.). The benchmark against data found in literature about the collapse of a slab under melting and partial vaporization under low/moderate heat loads encourages a further development of it. No gas kinetics has been included at this stage. When applied to a W PFC withstanding heat loads typical of a DVDE, the zero-order Matlab code predicts a depth of 20 mm (at least) far away from the irradiated surface, where the cooling system could be potentially considered safe, although the physics behind vaporization and the way it affects the energy balance needs a better understanding and implementation. The ongoing work is moving towards this direction, by looking at both the computational Lagrangian-Eulerian approach already implemented in Multi-physics software and experimental feedback, and the next step development will be explained in a future companion paper.

ACKNOWLEDGEMENT

This work has been carried out within the framework of the EURO*fusion* Consortium and has received funding from the Euratom research and training programme 2014-2018 and 2019-2020 under grant agreement No 633053. The views and opinions expressed herein do not necessarily reflect those of the European Commission.

REFERENCES

[1] M.L. Richiusa, W. Arter, D. Calleja, M. Firdaouss, J. Gerardin, M. Kovari, F. Maviglia, and Z. Vizvary. Bare and limiter DEMO single module segment concept first Wall misalignment study by 3D field line tracing. *Fusion Engineering and Design*, 160, 2020.

[2] F. Maviglia, C. Bachmann, G. Federici, T. Franke, M. Siccinio, C. Vorpahl, R. Albanese, R. Ambrosino, E. Fable, M. Firdaouss, J. Gerardin, V.P. Loschiavo, M. Mattei, F. Palermo, M.L. Richiusa, F. Villone, and Z. Vizvary. Impact of plasma thermal transients on the design of the EU DEMO first wall protection. *Fusion Engineering and Design*, 158(April):111713, sep 2020.

[3] P. C. Stangeby and R. Mitteau. Analysis for shaping the ITER first wall. *Journal of Nuclear Materials*, 390-391(1):963–966, 2009.

[4] W. Arter, V. Riccardo, and G. Fishpool. A CAD-based tool for calculating power deposition on tokamak plasma-facing components. *IEEE Transactions on Plasma Science*, 42(7):1932–1942, jul 2014.

[5] H.S. Carslaw and J.C. Jaeger. *Conduction of Heat in Solids*. Oxford science publications. Clarendon Press, 1986.

[6] J. Crank. *Free and Moving Boundary Problems*. Oxford science publications. Clarendon Press, 1987.

[7] H. Hu and S.A. Argyropoulos. Mathematical modelling of solidification and melting : a review. 4:371–396, 1996.

[8] C. Vilas, A.A. Alonso, E. Balsa-Canto, E. Lopez–Quiroga, I.C. Trelea. Model-based real time operation of the freeze-drying process. *Processes*, 8(3), 2020.

[9] T. C. Illingworth and I. O. Golosnoy. Numerical solutions of diffusion-controlled moving boundary problems which conserve solute. *Journal of Computational Physics*, 209(1):207–225, 2005.

[10] H.G. Landau. Heat conduction in a melting solid. *Quarterly of Applied Mathematics*, 8(1):81–94, 1950.

[11] M. Zerroukat. A Boundary Element Method for Multiple Moving Boundary Problems. 519:501–519, 1997.

[12] F. Maviglia, C. Bachmanna, G. Federici, T. Franke, M. Siccinio, R. Albanese, R. Ambrosino, W. Arter, R. Bonifetto, G. Calabr, R. De Luca, L.E. Di Grazia, E. Fable, P. Fanelli, A. Fanni, M. Firdaouss, J. Gerardin, R. Lombroni, M. Mattei, M. Moscheni, W. Morris, G. Pautasso, S. Pestchanyi, G. Ramogida, M.L. Richiusa, G. Sias, F. Subba, F. Villone, J. You, and Z. Vizvary. Integrated design strategy for EU-DEMO first wall protection from plasma transients *Paper under revision in Fusion Engineering and Design*.